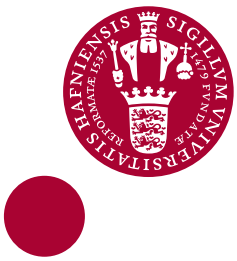

Combined Staining Techniques for Demonstration of Staphylococcus aureus Biofilm in Routine Histopathology

Jensen, Louise Kruse; Henriksen, Nicole Lind; Bjarnsholt, Thomas; Kragh, Kasper Nørskov; Jensen, Henrik Elvang

Published in:
Journal of Bone and Joint Infection

DOI:
10.7150/jbji.22799

Publication date:
2018

Document version
Publisher's PDF, also known as Version of record

IVYSPRING INTERNATIONAL PUBLISHER

Journal of Bone and Joint Infection

2018; 3(1): 27-36. doi: 10.7150/jbji.22799

Research Paper

Combined Staining Techniques for Demonstration of *Staphylococcus aureus* Biofilm in Routine Histopathology

Louise Kruse Jensen[1]✉, Nicole Lind Henriksen[1], Thomas Bjarnsholt[2,3], Kasper Nørskov Kragh[2], Henrik Elvang Jensen[1]

1. Department of Veterinary Clinical and Animal Sciences, Ridebanevej 3, 1870 Frederiksberg C, University of Copenhagen, Denmark
2. Costerton Biofilm Center, Department of Immunology and Microbiology, Blegdamsvej 3B, 2200 Copenhagen N, University of Copenhagen, Denmark
3. Department of Clinical Microbiology, Juliane Maries Vej 22, 2100 Copenhagen Ø, Copenhagen University Hospital, Denmark

✉ Corresponding author: Louise Kruse Jensen, Department of Veterinary Clinical and Animal Sciences, Ridebanevej 3, 1870 Frederiksberg C, University of Copenhagen, Denmark. Tel.: +45 22165332; Email: louise-k@sund.ku.dk

Received: 2017.09.12; Accepted: 2018.01.19; Published: 2018.02.20

Abstract

Aim: Visualization of *Staphylococcus aureus* biofilm using histochemical staining and combined histochemistry (HC) and immunohistochemistry (IHC).

Methods: The ability of *S. aureus* S54F9 to form biofilm was tested *in vitro*. Hereafter, infected bone tissue was collected from two different porcine models of osteomyelitis inoculated with *S. aureus* strain S54F9. The infection time was five and fifteen days, respectively. Twenty-five different histochemical staining protocols were tested in order to find the stains that could identify extracellular biofilm matrix. Protocols with an optimal visualization of biofilm extracellular matrix were combined with an immunohistochemical protocol based on a specific antibody against *S. aureus*. The combined protocols were applied to the tissue from the porcine models and to infected bone tissue from a child suffering from chronic staphylococcal osteomyelitis for more than a year.

Results: *S. aureus* S54F9 showed an ability to form biofilm *in vitro*. Visualization of biofilm, *i.e.* bacterial cells and extracellular matrix in different colours, was seen when the immunohistochemical protocol was combined with Alcian Blue pH3, Luna and Methyl-pyronin green. The bacterial cells were red to light brown and the extracellular matrix either light blue, blue or orange depending on the histochemical stain. In the porcine models and the human case 10 and 90 percent, respectively, of the bacterial aggregates in a 100x magnification field displayed both the extracellular matrix and the bacterial cells simultaneously in two different colours.

Conclusions: A combination of HC and IHC can be used to diagnose and characterise biofilm infections on a routine basis.

Key words: Biofilm, *Staphylococcus aureus*, bone infection, histology, light microscopy

Introduction

Bacterial biofilms are microbial derived communities, characterized by aggregates of bacterial cells that are attached to a substratum/interface or to each other and embedded in a matrix of extracellular polymeric substances [1-3]. Furthermore, the bacteria exhibit an altered phenotype in regard to growth, gene expression and protein production [2,3] and show increased tolerance towards antibiotics and the host immune system [3]. In most *in-vitro* biofilms, the bacteria account for less than 10 % of the dry mass, whereas the extracellular matrix can account for more than 90 % [4]. The extracellular matrix of a biofilm is composed of molecules produced both by the bacteria and the host and includes polysaccharides, structural proteins, enzymes, nucleic acids and lipids [4]. All the different molecules have specific roles in favour of the

survival and growth of the embedded bacteria (Table 1) [4]. Despite extensive research focusing on bacterial biofilms, a comprehensive analysis of which histochemical stains that can identify the components of the extracellular biofilm matrix is lacking. Therefore, pathologists are often not aware of the presence of biofilm formation when examining slides for diagnosing bacterial infection in routine diagnostic laboratories.

Table 1. Function of major components of extracellular matrix (ECM) in bacterial biofilms, modified from [4].

Component	Function
Polysaccharides and proteins	-Adhesion between biofilm components and surfaces -Aggregation and immobilization of bacterial cells -Polysaccharide-enzyme binding causing accumulation, retention and stabilization of enzymes -Cohesion of biofilms ensuring mechanical stability, architecture and cell communication -Enzymatic activity (just proteins) -Electron donor or acceptor, permitting redox activity within the biofilm matrix (just proteins) -Nutrient source for utilization by biofilm cells -Protective barrier conferring host defenses against infection and tolerance to antimicrobials -Retention of water providing a hydrated microenvironment -Promoting nutrient accumulation and detoxification of xenobiotics -Promoting ion exchange, mineral formation, detoxification of toxic metal ions and polysaccharide gel formation
Nucleic acids	-Adhesion between biofilm components and surfaces -Aggregation and immobilization of bacterial cells -Cohesion of biofilms ensuring mechanical stability, architecture and cell communication -Exchange of genetic information between biofilm cells -Nutrient source for utilization by biofilm cells
Lipids	-Adhesion between biofilm components and surfaces (amphiphilic molecules) -Nutrient source for utilization by biofilm cells

Biofilm formation facilitates bacterial tolerance to elimination by antimicrobial agents, host phagocytic clearance and host oxygen radicals and proteases [5]. Therefore, biofilms are difficult to eradicate and present in many chronic diseases like cystic fibrosis, chronic wounds and orthopaedic infections [3]. In orthopaedics, biofilm has been identified inside necrotic bone tissue and on the surface of orthopaedic implants [4]. *Staphylococcus aureus* is one of the most common infectious agents in orthopaedics [5]. Recently, the porcine *S. aureus* strain S54F9 spa type t1333, originating from a porcine lung abscess [6], was characterized by whole-genome sequencing [7]. The strain has been used in various reproducible and discriminative porcine models of haematogenous osteomyelitis [8], implant-associated osteomyelitis [9], endocarditis [10] and sepsis [11]. Due to the infectious potential of *S. aureus* S54F9, its *in-vitro* production of biofilm was tested in the present study. Furthermore, histochemical stains, alone or combined with immunohistochemistry (IHC), were applied to tissue from experimental *S. aureus* S54F9 bone infections in pigs [8,9] and from a clinical *S. aureus* bone infection [12] in order to demonstrate *S. aureus* biofilm using light microscopy.

Materials and methods

In vitro biofilm formation

The ability of *S. aureus* S54F9 to form biofilm was tested in a microtiter biofilm assay system as described by O'toole [13]. Both *S. aureus* S54F9 and *S. aureus* RN4220 (a reference strain) [14] were diluted to a final cell density of OD 0.005 in TSB (Sigma, USA) with 1% glucose. Of this solution, 150 µl was applied to each well of a 96-well microtiter plate (Thermo Fisher, USA). Plates were incubated for 24 hours at 37˚C. After incubation the content was gently removed by inverting the plate. The wells were gently rinsed by adding 200 µl saline (0.9%) to each well. In order to fixate biomass, 180 µl methanol (Sigma, USA) was added to each well for 15 min. For staining, 180 µl Crystal Violet solution (CV) (Sigma, USA) was applied to the wells for 15 min. Two wells were left unstained for microscopy. The CV solution was removed by inverting the plate. Residue CV was removed by gently rinsing each well with 200 µl saline (0.9%). The plate was air-dried at room temperature. Bound CV was expelled by incubating the plate in 180 µl 96.5% (V/V) EtOH for 15 min. The intensity of the CV staining was evaluated by OD measuring at 594 nm on a VictorX4 plate reader (Perkin Elmer, USA). A t-test was used to show differences in OD measurements between the two *S. aureus* strains. For confocal microscopy, biofilm in the two CV unstained microtiter wells was stained with 0.3mM Syto9 (Molecular Probes, USA) and incubated for 15 min. Microscopy was performed using an inverted Zeiss LSM 880 confocal microscope running the program Zen 2.1 (Ziess, Germany). Images were obtained with a 488 nm laser with an emission peak at 498-501 nm by using a 10x/0.3 and a 63x/1.4 objective. 3D projections of these images were produced using the program Imaris (Bitplane, Switzerland).

Sampling of porcine bone tissue

Two blocks of formalin-fixed, decalcified and paraffin embedded porcine infected bone tissue were used [9]. The first block contained tissue from a female pig inoculated with 10^4 CFU of *S. aureus* S54F9 locally in the right tibia followed by insertion of a small steel implant (2x15 mm). The pig was euthanized following five days of inoculation [9]. The tissue block included the implant cavity and the surrounding infected metaphyseal (trabecular) bone tissue (Figures 1A + 1B). The second block originated from a female pig inoculated with 10^4 CFU/kg BW of

S. aureus S54F9 into the right femoral artery [8]. This pig was euthanized following 15 days of inoculation [8]. The tissue block was sampled from a bone lesion in the distal metaphysis of the right femur (Figures 1C + 1D).

Sampling of human bone tissue

One block of formalin fixed, decalcified and paraffin embedded infected bone tissue from a 5 year-old boy with chronic, haematogenous osteomyelitis in the right femur, lasting for more than one year, was used [12]. The block had been sampled during therapeutic surgery and contained a large cortical sequester (Figures 1E + 1F). Microbiological testing demonstrated *S. aureus* as the infecting organism [12].

Histochemistry (HC)

Tissue sections of 4-5 µm from each of the two cases of porcine osteomyelitis and from the human case of osteomyelitis were stained with haematoxylin and eosin (HE). The HE stained sections of the lesions were used to describe the pathomorphology with regards to bone destruction, inflammatory cells and localization of bacteria. Furthermore, 25 consecutive sections of 4-5 µm were cut from both blocks of porcine tissue and stained with the HC stains listed in Table 2. For all stains, the colour of bacterial clusters and the ability to visualize an extracellular biofilm matrix were recorded. Furthermore, the level of contrast between the colour of the bacterial clusters and surrounding tissue (background) was scored: poor contrast (+), fair contrast (++), good contrast (+++).

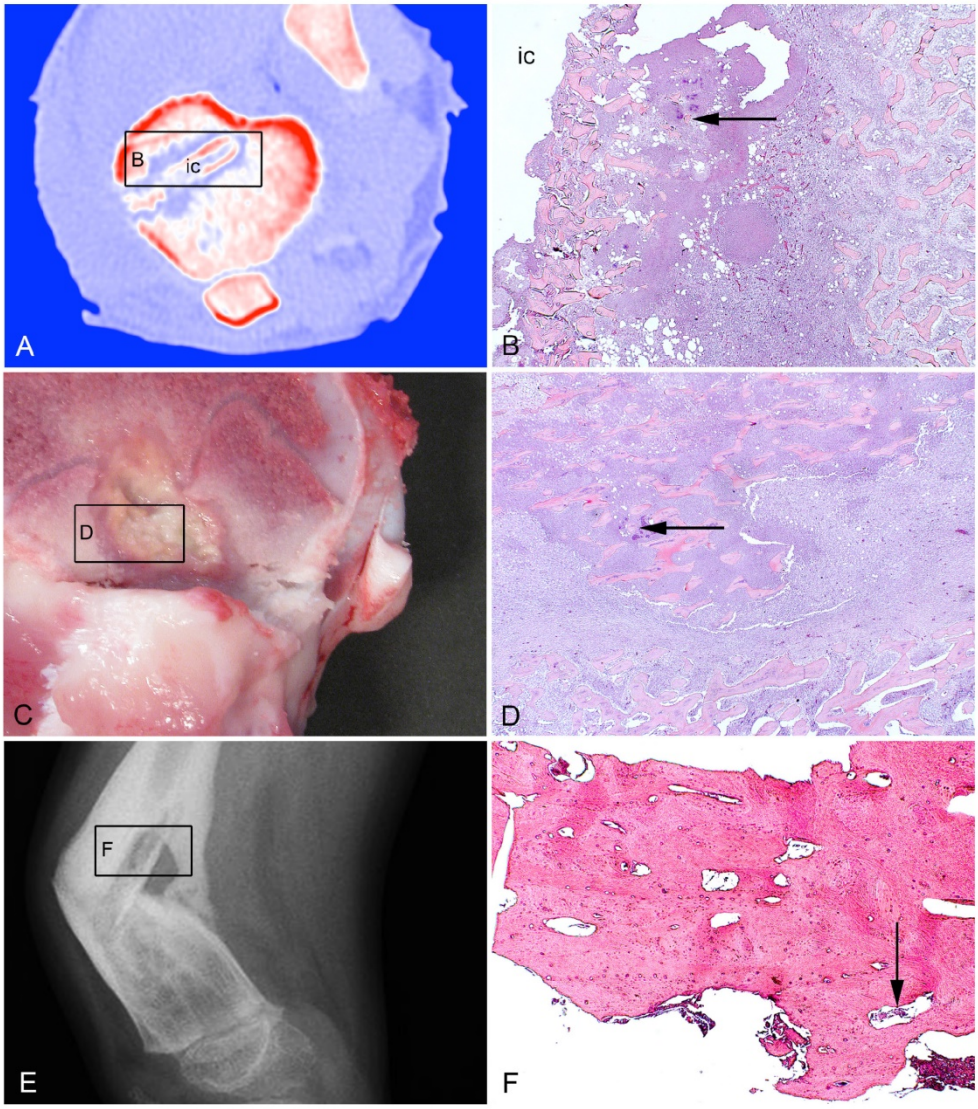

Figure 1. Bone tissue used in the present study. A: Porcine model of implant-associated osteomyelitis. CT scan after five days of inoculation demonstrating the tibial implant cavity (ic) used for injection of *S. aureus* and insertion of a small steel implant. B: Histology of picture A demonstrating bacteria (arrow) in the peri-implant tissue adjacent to the implant cavity (ic). HE. C: Porcine model of haematogenous osteomyelitis euthanized fifteen days after inoculation. A lesion is shown in the right femoral metaphysis. D: Histology of picture C demonstrating bacteria (arrow) centrally in the lesion. HE. E: X-ray of a child with haematogenous osteomyelitis and pathological fracture in the right femur. F: Histology of picture E demonstrating bacteria (arrow) in a cortical sequester. HE.

Table 2. Results of 25 histochemical stains, modified from the cited references, applied to bone tissue from porcine models of haematogenous and implant associated osteomyelitis induced with *Staphylococcus aureus* S45F9.

Stain	Staining pattern	Bacteria color	Matrix	Contrast	Protocol Reference
Connective tissue stains					
Alkaline congo red	Red: Amyloid (via. H-bonds), elastic fibers, eosinophil granules Blue: Nuclei	Purple	No	++	15
Crystal violet	Red-purple: Amyloid, mucin, renal hyaline Blue: Background	Purple	Yes Purple	++	15
Gomori's reticular fibers	Black: Reticular fibers Gray: Nuclei	Brown/purple	No	+	15
Luna	Red: Eosinophils, RBC (red blood cells) Blue: Background	Blue	Yes Blue	+++	16
Martius scarlet blue	Blue: Nuclei, collagen, (old fibrin) Yellow: RBC, (early fibrin) Red: Muscle, fibrin	Purple	No	+	15
Masson-trichome	Blue/black: Nuclei Red: Cytoplasm, muscle, RBC Blue: Collagen	Brown/purple	No	++	15
Picro-sirius red	Red: Collagen type 1-3, keratohyalin granules Polarized light: Collagen 1 – yellow/orange/red, collagen 3 - green	Orange	Yes Orange	++	17
PTAH	Dark blue: Muscle striations, neuroglia, fibrin, amoebae Blue: Nuclei, cilia, RBC Light blue: Myelin Deep red-brown: Collagen, osteoid, cartilage, elastic fibers Pale pink-brown: Cytoplasm	Brown/purple	No	+	16
Van Gieson	Blue/black: Nuclei Red: Collagen	Brown	No	+	15
Verhöeff's	Black: Elastic tissue fibers	Purple	No	+	15
Carbohydrate stains					
Alcian blue ph1	Blue: Acid mucins, proteoglycans, hyaluronic acid Red: Nuclei	Blue	Yes Blue	+	15
Alcian blue ph3	Blue: Acid mucins, proteoglycans, hyaluronic acid Red: Nuclei	Blue	Yes Blue	+++	15
PAS	Magenta: Glycogen, neutral/sialomucins, glycoproteins Blue: Nuclei	Purple	Yes Purple	++	15
Safranin O	Black: Nuclei Grey/green: Cytoplasm Orange/red: Cartilage, mast cells	Purple	Yes Purple	+++	18
Toluidine blue-acetone	Blue/purple: Mast cell granula Blue: Nuclei and background	Blue	Yes Blue	++	15
Lipid stains					
Oil-red O	Red: Fat Blue: Nuclei	Purple	Yes Purple	++	15
Pigment and mineral stains					
Perls' Prussian blue	Blue: Ferric iron Red: Nuclei	Red	No	++	15
Von kossa	Black: Mineralized bone Red: Osteoid	Brown	No	+	15
Alizarin red S	Orange-red: Calcium deposits (especially small deposits)	Yellow/brown	No	+/++	15
Microorganism stains					
Giemsa	Dark blue: Protozoa, microorganisms Pink-pale blue: Background Blue: Nuclei	Blue	Yes Blue	+++	15
Grocott methenamine-silver	Black: Fungi, pneumocystis, melanin, hyphae, yeast form cells of fungi Taupe-dark gray: Mucins, glycogen Pale green: Background	Black	No	++	15
Levaditis	Black: Spirochaetes, some organisms and fungi Yellow: Background	Black	No	++	16
Gram	Blue/black: Gram positive bacteria Red: Gram negative bacteria	Purple/blue	Yes Purple/blue	+++	15
Nucleic acid stains					
Feulgen nuclear reaction for DNA	Red/purple: DNA Green: Cytoplasm	Turquoise	No	+	15
Methyl green-pyronin	Green/blue: DNA Red: RNA	Red/pink	Yes Red/pink	+++	15

Contrast: poor contrast (+), fair contrast (++), good contrast (+++) between bacteria and background.

Immunohistochemistry (IHC) towards *S. aureus*

Porcine and human tissue sections of 4-5 µm were prepared and processed for indirect *in situ* identification of *S. aureus*. Primary *S. aureus* specific antibodies (ab37644, Abcam, Cambridge, UK, diluted 1:2000 in 5% swine serum) targeting at antigen protein A were used. The specific protocol has recently been described (see also next section) [19]. The three smallest and three largest (diameter) IHC positive bacterial aggregates were measured using the software Delta Pix Insight (Smørum, Denmark).

Combined IHC and HC

HC stains demonstrating extracellular biofilm matrix and good contrast to the surrounding tissue (Table 2) were selected to be combined with IHC towards *S. aureus*. Consecutive tissue sections of 4-5 µm from the porcine and human tissue blocks were mounted on adhesive glass slides (Thermo Scientific, Menzel GmbH & CoKG, Baunschweig, Germany). Following deparaffinization, antigen retrieval procedures were carried out by treatment with a Trypsin solution (Sigma-Aldrich, St. Louis, Missouri, USA) pH 7.8 for 30 min at 37 °C. This was followed by blocking of endogenous peroxidase by 0.6% H_2O_2 for 15 min and blocking of unspecific protein binding by Ultra V Block (AH-diagnostics, Aarhus, Denmark) for five min. Tissue sections were incubated with the primary antibodies overnight followed by the application of a primary antibody enhancer, horseradish peroxidase polymer and aminoethylcabazol/3,3'-diaminobenzidine as described by the manufacturer (AH-diagnostics, Aarhus, Denmark). Throughout the immune-staining protocol, tissue sections were washed in Tris-buffered saline pH 7.6. After the IHC steps, the HC protocols with good contrast (Table 2) were applied, and all tissue sections were mounted with glycerol–gelatin and a cover slip. For each of the porcine and human tissue sections stained with the combined IHC and HC protocols, the number of bacterial aggregates with and without a visible biofilm matrix were registered in a 100x magnification field.

Image analysis

Combined IHC and HC stained porcine and human tissue sections were scanned using Zeiss Axio Scan.Z1 at a 10x objective and imported into Visiopharm Integrator System 4.6.857. The Visiopharm software was trained to recognize and stain positive areas of *S. aureus* (yellow) and extracellular matrix (purple). Pre-processing median filters for red/green/blue bands and the bayessian classification method were applied to improve image quality and recognition ability. On each tissue section, a representative bacterial aggregate demonstrating both bacterial cells and extracellular matrix was outlined. The Visiopharm software was used to identify and calculate the percentage of *S. aureus* and extracellular matrix positive areas within the outlined bacterial aggregate.

Results

In vitro biofilm formation

S. aureus S54F9 produced the same amount (P = 0.4693) of attached biomass as the known biofilm producing strain RN4220 (Figure 2A). A dense layer of biomass was visible in the bottom of the microtiter trays wells. At a higher magnification (630x), a compact layer of coccid bacteria comparable to *S. aureus* was seen (Figure 2B) [13,20].

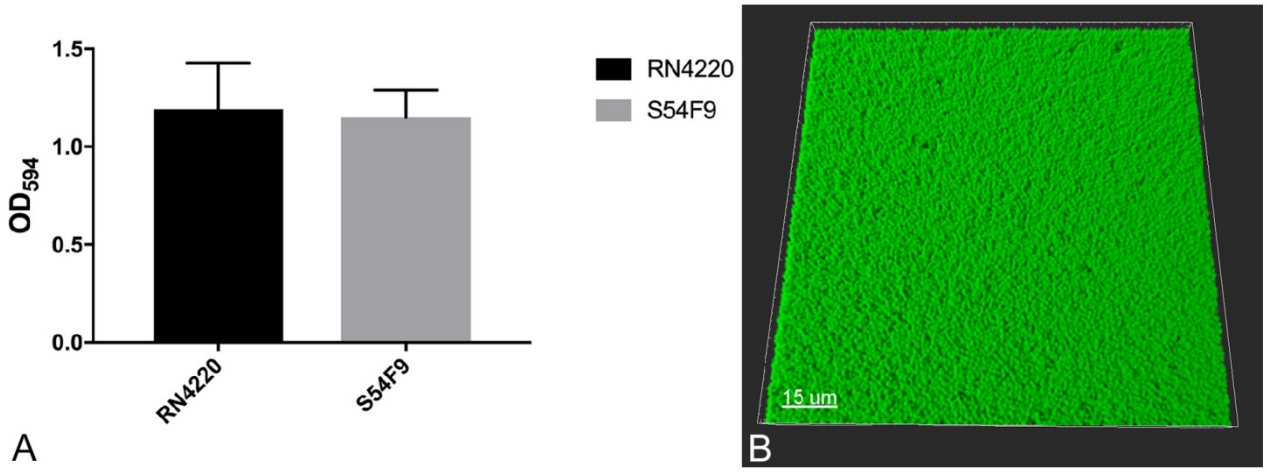

Figure 2. Biofilm formation *in vitro*. A: Attached biomass of reference strain RN4220 and S54F9 in the wells of microtiter trays based on the binding of crystal violet. Mean OD_{594} with SEM. B: 3D projection of the bottom of a microtiter well stained for bacterial cells with green Syto9. 630 x magnification.

Histochemistry

The porcine (5 day) tibial lesion consisted of necrotic trabecular bone debris, intermingled with accumulations of neutrophilic granulocytes and bacterial aggregates (Figure 1B). The porcine (15 day) femoral lesion consisted centrally of sequestered trabecular bone tissue with empty lacuna. The dead bone tissue was surrounded by neutrophilic granulocytes and aggregates of bacteria (Figure 1D). Macrophages and fibroblasts encapsulated the area (Figure 1D). The human tissue consisted of necrotic cortical bone tissue. The lamellar cortical bone structure could be observed in the sequestrum, and aggregates of bacteria and few inflammatory cells were located within Volkmann canals and the Haverisian system (Figure 1F). In the porcine tissues, six HC stains (Table 2) revealed the presence of an extracellular biofilm matrix and good contrast to the surrounding tissue (Figures 3B-F, Table 2).

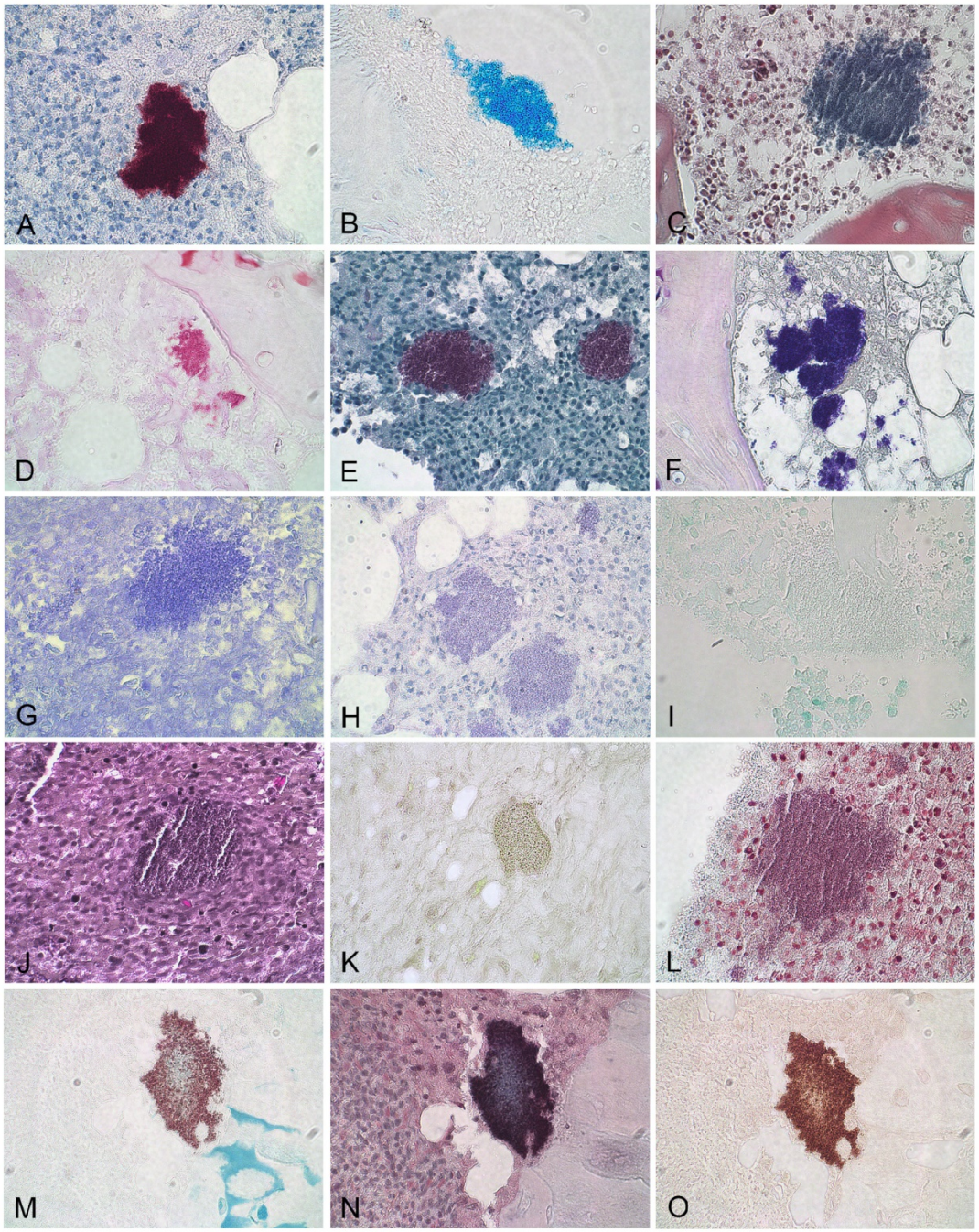

Figure 3. Immunohistochemical (A), histochemical (B-L) and combined histochemical/immunohistochemical (M-O) stains applied to porcine *S. aureus* infected bone tissue. A: *S. aureus* immunohistochemistry, B: Alcian blue pH3, C: Luna, D: Methyl green-pyronin, E: Safranin O, F: Gram, G: Crystal Violet, H: Oil red, I: Feulgen, J: Verhoeff, K: Alzian Red, L: Masson trichome, M: Alcian blue pH 3 + *S. aureus* immunohistochemistry, N: Luna + *S. aureus* immunohistochemistry, O: Methyl green-pyronin + *S. aureus* immunohistochemistry. All pictures are at 60x magnification

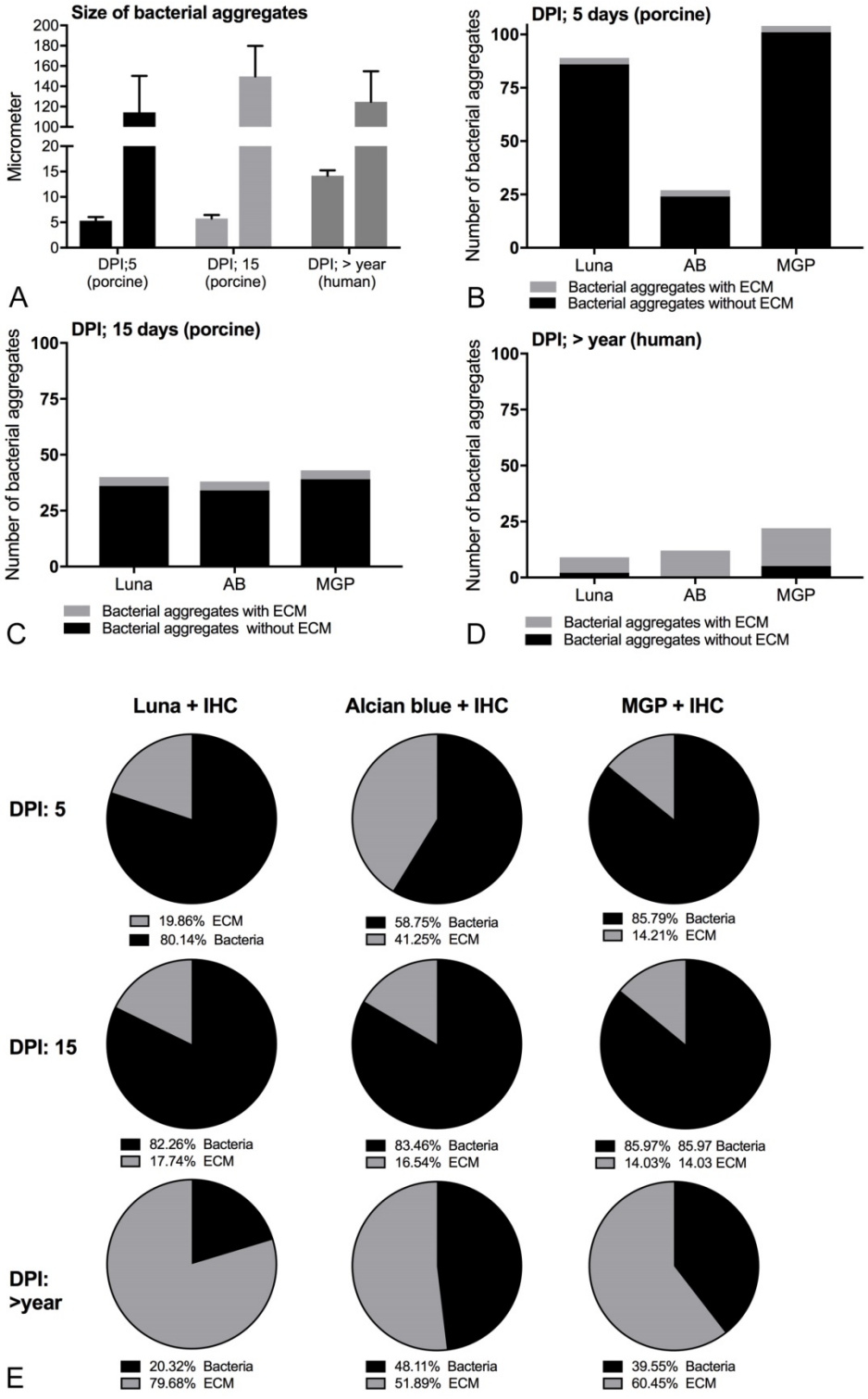

Figure 4. Composition and size of biofilm forming infections in porcine and human bone tissue. A: Size of the three smallest and three largest bacterial aggregates seen with immunohistochemistry towards *S. aureus*, Mean ± SD. B-D: Number of bacterial aggregates with and without a visible extracellular biofilm matrix at 100x magnification following combined histochemistry with immunohistochemistry. The x-axis shows the histochemical stains. E: Percentage of bacterial cells and extracellular matrix in single representative *S. aureus* biofilm aggregates. AB: Alcian Blue pH3, MGP: Methyl-pyronin green, DPI: days post infection, ECM: extracellular matrix.

Immunohistochemistry towards *S. aureus*

IHC staining towards *S. aureus* successfully demonstrated the presence of *S. aureus* in both porcine and human bone tissue (Figure 3A). Positive *S. aureus* bacteria were stained red. The size of the three smallest and three largest bacterial aggregates are shown in Figure 4A.

Combined immunohistochemistry and histochemistry

Of the six HC stains with good contrast and visible biofilm matrix, Alcian blue pH 3, Luna and Methyl green-pyronin (Table 2) were found to be optimal for combination with IHC. The remaining three good HC stains, *i.e.* Safranin O, Giemsa and Gram (Table 2) resulted in purple or blue bacterial aggregates which combined with IHC resulted in a brown indefinite mass. Alcian blue pH3, Luna or Methyl green-pyronin combined with IHC stained the bacterial cells red to light brown and the extracellular matrix light blue, blue or orange, respectively (Figures 3M-O). Extracellular matrix and bacteria were simultaneously seen in 3-10 % and 80-100 % of the bacterial aggregates in the porcine and human bone tissue, respectively (Figures 4B-D). For the single representative bacterial aggregates used to determine the bacterial cell/extracellular matrix ratio, a higher ratio of extracellular matrix than bacterial cells was seen in the human tissue compared to the two porcine models (Figure 4E and Figure 5).

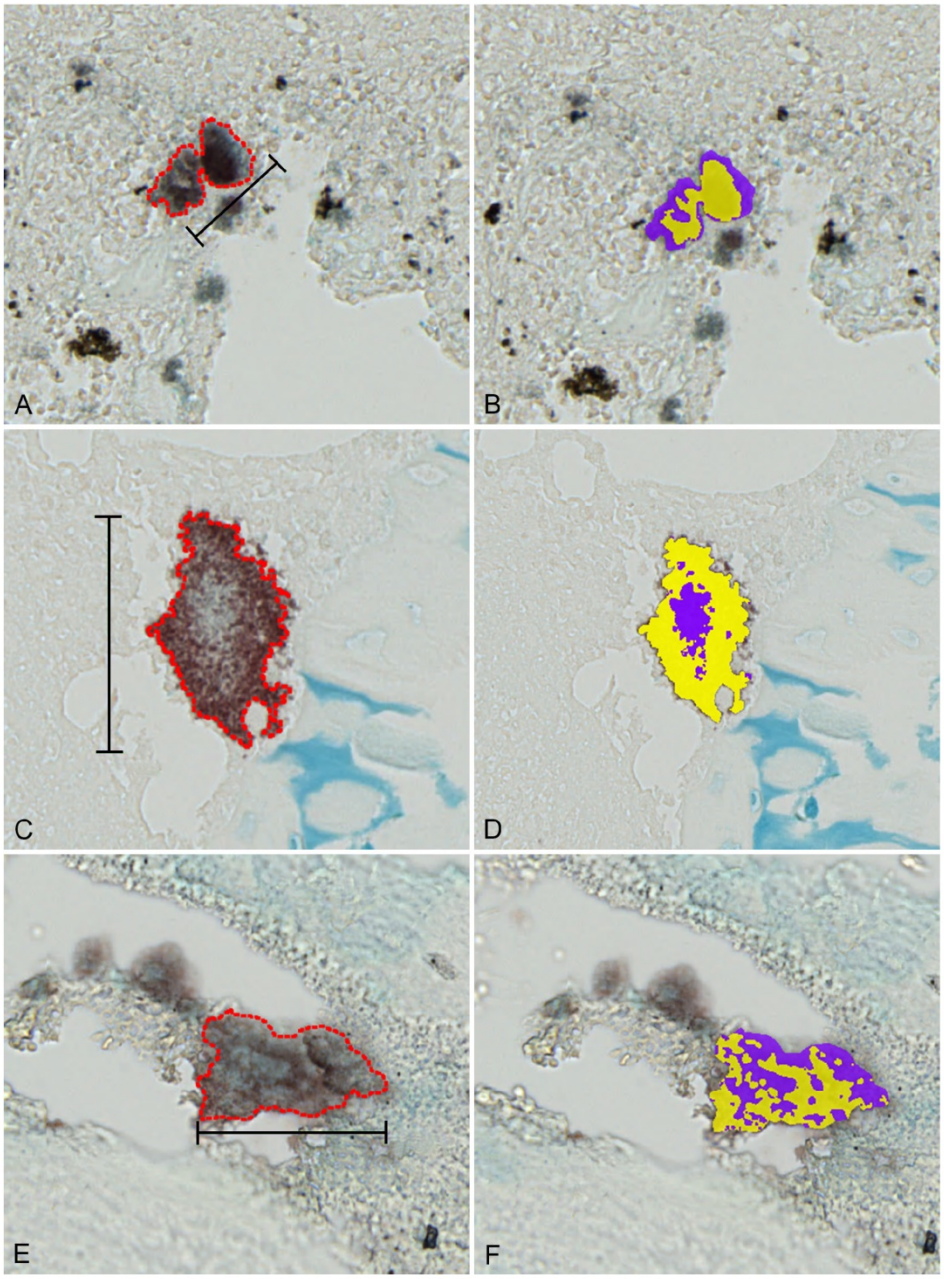

Figure 5. Percentage of bacteria and extracellular matrix in *S. aureus* biofilm infections. Left column: combined immunohistochemistry (towards *S. aureus*) and Alcian blue pH3 staining of representative bacterial biofilms (red outline) displaying both bacteria (red/brown) and extracellular matrix(blue). Right column demonstrates calculations of % bacterial cells (yellow) and extracellular matrix (purple). A+B: Bone tissue from a porcine model of *S. aureus* implant-associated osteomyelitis infected for five days. Bar = 40 μm. C+D: Bone tissue from a porcine model of *S. aureus* haematogenous osteomyelitis infected for fifteen days. Bar = 78 μm. E+F: Bone tissue from a patient suffering from *S. aureus* haematogenous osteomyelitis for more than one year. Bar = 72 μm.

Discussion

Biofilm is typically found in chronic infections, which means that the infection persists despite adequate antibiotic therapy and host immune defence mechanisms [21]. Therefore, increased focus has been on diagnosing and treating bacterial biofilm infections [21]. In the present study, *S. aureus* S54F9 showed the ability to form biofilm *in vitro*. The histochemically stained bacterial aggregates seen in the porcine osteomyelitis models (inoculated with S54F9), therefore, likely represent *in vivo* biofilm produced by *S. aureus* S54F9. Likewise, the HC and IHC double coloured bacterial clusters seen in the human tissue also represent biofilm produced by *S. aureus.*

Recently, ESCMID (European Society for Clinical Microbiology and Infectious Diseases) published guidelines for diagnosing biofilm infections [21]. According to these guidelines, biofilm detection requires that tissue microscopy shows evidence of an infective process, such as the presence of leucocytes, and that the microorganisms present form aggregates embedded in a self-produced matrix distinct from the surrounding tissue [21]. These requirements were achieved with the present combination of HC and IHC staining's for light microscopy. Light microscopy is one of the most common methods by which bacteria are demonstrated in tissue [22]. Bacteria can be visualized in routine HE stains, although a disadvantage of HE staining is that haematoxylin stains all nucleic acids, which may make it difficult to distinguish microbial cells from host cells [22]. To specifically detect bacteria with HC stains, the Gram stain can be used [15]. HC stains are commonly used to demonstrate different molecules in tissue sections based on chemical properties. Therefore, it is reasonable to suggest that the biofilm extracellular matrix can be visualized by different HC stains due to its content of carbohydrates, proteins, lipids and nucleic acids (Table 2). A limited number of studies demonstrating bacterial biofilm by HC and light microscopy exists [23-25]. In these studies, PAS, Giemsa, Gram or HE stains have been applied to demonstrate bacterial biofilms [23-25]. Also more advanced microscopic techniques have been used to visualize biofilm, *e.g.* confocal laser scanning microscopy, fluorescence microscopy, scanning electron microscopy, and transmissions electron microscopy [26]. A combination of confocal microscopy and reverse transcriptase-polymerase chain reaction has been described as a powerful tool for detection of biofilms in operative tissue specimens [27]. Confocal laser scanning microscopy and electron microscopy are, however, specialized and time consuming techniques based on equipment not generally available in diagnostic laboratories [28].

Although the present combinations of HC and IHC protocols were able to demonstrate biofilm formation by *S. aureus*, a negative result can not exclude the presence of biofilm. Furthermore, one should be aware of the fact that extracellular biofilm matrix components differ amongst different bacteria and bacterial strains. In a clinical situation, a combined staining technique can not be applied before the results of microbiology are available in order to select adequate antibodies for IHC. Therefore, the introduction of combined HC and IHC staining, as demonstrated in this study, is not useful in facilitating fast histopathological diagnosis of infections. However, it is useful for facilitating the demonstration of bacterial biofilm formation, which may impact the selected treatment protocol. Histologically, diagnosis of bone infection should not rely only on bacterial identification, but also on the patho-morphology present.

Biofilm extracellular matrix components include polysaccharides, lipids, proteins and extracellular DNA (Table 1). The light blue colour of the biofilm matrix seen with the Alcian Blue pH3 stain is due to a chemical reaction with polysaccharides. The blue and orange colours of biofilm matrix seen with Luna and Methyl-green pyronin, respectively, are due to haematoxylin and methyl-green which both stain nucleic acids. Extracellular DNA has been identified as a major structural component in the biofilm matrix of *S. aureus*, whereas it is only a minor component of biofilm formed by *S. epidermidis* [29]. In a review concerning biofilm formation *in vivo*, it was recently shown that tissue biofilm aggregates in chronic infections of humans, including orthopaedic infections, despite anatomical location and type of bacteria involved have an upper size limit of approximately 200 μm [30]. None of the measured bacterial aggregates in the present study exceeded this limit. According to Bjarnsholt et al. [30] and Parsek et al. [31] the human osteomyelitis case of the present study fulfils all criteria for a biofilm infection. This includes tissue adherent pathogenic bacteria found in clusters with a diameter within the range of ~5-200 μm [30], infection localized to a particular anatomic site and persistent infection despite exposure to antibiotics [30].

Conclusion

- The porcine *S. aureus* strain S54F9 has the ability to form biofilm both *in vitro* and *in vivo* and is, therefore, a reliable agent to be used in animal models of human chronic infectious diseases caused by *S. aureus.*
- A combination of HC and IHC can be used to

diagnose and characterise biofilm infections. Furthermore, a list of how biofilm is stained by histochemical stains available in most routine diagnostic laboratories is provided.

Abbreviations

IHC: immunohistochemistry; HC: histochemistry, CFU: colony-forming unit, OD: optical density; CV: Crystal Violet solution; HE: haematoxylin and eosin.

Acknowledgements

We would like to thank Betina Andersen and Elizabeth Petersen for excellent laboratory assistance and the Core Facility for Integrated Microscopy at The University of Copenhagen for assistance with scanning of tissue sections.

Funding

This study was financed by grant no. 4005-00035B from the Danish Research Council and the European Union's Horizon 2020 research and innovation program under NOMORFILM project grant agreement No 634588 and grant no. R173-2014-584 and R105-A9791 from the Lundbeck Foundation to TB.

Ethical Approval

The porcine tissue blocks were collected from studies [8,9] approved by the Danish Animal Experimental Act (Licence no. 2013/15-2934-00946 and 2008/561-37). The human tissue block was collected from a study [12] approved by the Danish National Committee on Biomedical Research Ethics (Protocol no. H-2-2011-102).

Competing Interests

The authors have declared that no competing interest exists.

References

1 Costerton JW, Geesey GG, Cheng K-J. How bacteria stick. Sci Am. 1978; 238: 86-95.
2 Donlan RM, Costerton WJ. Biofilms: survival mechanisms of clinically relevant microorganisms. Clin Microbiol Rev. 2002; 15: 167-193.
3 Bjarnsholt T. The role of bacterial biofilms in chronic infections. APMIS. 2013; 121: 1-51.
4 Flemming H-C, Wingender J. The biofilm matrix. Nature Rev Microbiol. 2010; 8: 623-633.
5 Brady RA, Leid JG, Calhoun JH, et al. Osteomyelitis and the role of biofilms in chronic infection. FEMS Immunol Med Microbiol. 2008; 52: 13-22.
6 Hasman H, Moodley A, Guardabassi L, et al. *spa* type distribution in *Staphylococcus aureus* originating from pigs, cattle and poultry. Vet Microbiol. 2010; 141: 326-331.
7 Aalbæk B, Jensen LK, Jensen HE, et al. Whole-genome sequence of *Staphylococcus aureus* S54F9 isolated from a chronic disseminated porcine lung abscess and used in human infection models. Genome Announc. 2015; 3: 1-2.
8 Johansen LK, Koch J, Frees D, et al. Pathology and biofilm formation in a porcine model of staphylococcal osteomyelitis. J Comp Path. 2012; 147: 343-353.
9 Jensen LK, Koch J, Dich-Jorgensen K, et al. Novel porcine model of implant-associated osteomyelitis: A comprehensive analysis of local, regional and systemic response. J Orthop Res. 2017; doi: 10.1002/jor.23505: 1-11.
10 Christiansen JG, Jensen HE, Johansen LK, et al. Porcine models of non-bacterial thrombotic endocarditis (NBTE) and infective endocarditis (IE) caused by *Staphylococcus aureus*: A preliminary study. J Heart Valve Dis. 2013; 22: 368-376.
11 Sørensen KE, Skovgaard K, Heegaard PMH et al. The impact of *Staphylococcus aureus* concentration on the development of pulmonary lesions and cytokine expression after intravenous inoculation of pigs. Vet Pathol. 2012; 49: 950-962.
12 Johansen LK, Koch J, Kirketerp-Møller K, et al. Therapy of haematogenous osteomyelitis – a comparative study in a porcine model and Angolan children. In vivo. 2013; 27: 305-312.
13 O'Toole GA. Microtiter dish biofilm formation assay. J Vis Exp. 2011; doi:10.3791/2437: 1-2.
14 Malone CL, Boles BR, Lauderdale KJ, et al. Flourescent reporters for *Staphylococcus aureus*. J Microbiol Methods. 2009; 77: 251-260.
15 Bancroft, J.D. & Gamble, M. Theory and practice of histological techniques. New York, USA: Churchill Livingstone Elsevier; 2008.
16 Luna LG. Manual of histologic and methods of the armed forces institute of pathology. New York, USA: McGraw-Hill; 1960.
17 Pearse SGE. Histochemistry theoretical and applied. New York, USA: Churchhill Livingstone; 1985.
18 Lille RD, Fullmer HM. Histopathologic technic and practical histochemistry. New York, USA: McGraw-Hill; 1965.
19 Johansen LK, Frees D, Aalbæk B, et al. A porcine model of acute, haematogenous localized osteomyelitis due to *Staphylococcus aureus*: a pathomorphological study. APMIS. 2011; 119: 111-118.
20 Yarwood JM, Bartels DJ, Volper EM, et al. Quorum sensing in *Staphylococcus aureus* biofilms. J Bacteriol. 2004; 186: 1838–1850.
21 Høiby N, Bjarnsholt T, Moser C, et al. ESCMID guideline for the diagnosis and treatment of biofilm infections 2014. Clin Microbiol Infect. 2015; 21: S1-S25.
22 Rumbaugh KP, Carty NL. In vivo models of biofilm infection. In: Bjarnsholt T, ed. Biofilm infections, 1st ed. New York: Springer-Verlag; 2011: 267-290.
23 Winther B, Gross BC, Hendley JO, et al. Location of bacterial biofilm in the mucus overlaying the adenoid by light microscopy. Arch Otolaryngol Head Neck Surg. 2009; 135: 1239-1245.
24 Hochstim CJ, Choi JY, Lowe D, et al. Biofilm detection with hematoxylin-eosin staining. Arch Otolaryngol Head Neck Surg. 2010; 136: 453-456.
25 Tóth L, Csomor P, Sziklai I, et al. Biofilm detection in chronic rhinosinusitis by combined application of hematoxylin-eosin and gram staining. Eur Arch Otorhinolaryngol. 2011; 268: 1455-1462.
26 Harrison-Balestra C, Cazzangia AL, Davis SC, et al. A wound-isolated *Pseudomonas aeruginosa* grows a biofilm in vitro within 10 hours and is visualized by light microscopy. Dermatol Surg. 2003; 29: 631-635.
27 Stoodley P, Nistico L, Johnson S et al. Direct demonstration of viable *Staphylococcus aureus* biofilms in an infected total joint arthroplasty. J Bone Joint Surg Am. 2008; 90: 1751-1758.
28 Izano EA, Amarante MA, Kher WB, et al. Differential roles of poly-N-acetylglucosamine surface polysaccharide and extracellular DNA in *Staphylococcus aureus* and *Staphylococcus epidermidis* biofilms. Appl Environ Microbiol. 2008; 74: 470-476.
29 Ziran BH. Osteomyelitis. J Trauma. 2007; 62: 59-60.
30 Bjarnsholt T, Alhede M, Alhede M, et al. The in vivo biofilm. Trends Microbiol. 2013; 21: 466-474.
31 Parsek MR, Singh PK. Bacterial biofilms: an emerging link to disease pathogenesis. Annu Rev Microbiol. 2003; 57: 677-701.